



OPEN ACCESS

EDITED BY Mingyi Xu, South China University of Technology, China

REVIEWED BY
Abobakr Sori,
Sahand University of Technology, Iran
Kam Ng,
University of Wyoming, United States

*CORRESPONDENCE
Emelie Crafoord

☑ Emelie.Crafoord@ltu.se

RECEIVED 13 August 2025 ACCEPTED 29 September 2025 PUBLISHED 31 October 2025

CITATION

Crafoord E, Wanhainen C and Bark G (2025) Permanent storage of carbon dioxide in mafic rock formations: exploring Sweden's potential.

Front. Clim. 7:1685187. doi: 10.3389/fclim.2025.1685187

COPYRIGHT

© 2025 Crafoord, Wanhainen and Bark. This is an open-access article distributed under the terms of the Creative Commons
Attribution License (CC BY). The use, distribution or reproduction in other forums is permitted, provided the original author(s) and the copyright owner(s) are credited and that the original publication in this journal is cited, in accordance with accepted academic practice. No use, distribution or reproduction is permitted which does not comply with these terms

Permanent storage of carbon dioxide in mafic rock formations: exploring Sweden's potential

Emelie Crafoord*, Christina Wanhainen and Glenn Bark

Division of Geosciences and Environmental Engineering, Department of Civil, Environmental and Natural Resources Engineering, Luleå University of Technology, Luleå, Sweden

Mineral carbonation in reactive bedrock offers a rapid and permanent method for carbon dioxide (CO₂) sequestration, converting CO₂ into stable mineral phases within a geologically short timeframe. This study presents the first-ever systematic assessment of onshore CO₂ mineral storage potential in Sweden, based on fieldwork, sampling, and mineralogical and geochemical analyses conducted at 23 localities. While this theoretical assessment cannot resolve uncertainties related to reactivity, dissolution capacity, and sequestration efficiency, it provides a critical foundation for identifying potentially favorable storage reservoirs. The findings highlight the Örnsköldsvik and Sundsvall areas in central Sweden, hosting a gabbro-anorthosite complex together with a set of dolerites, as the more suitable lithologies for onshore CO₂ storage. These rocks are distinguished by their high content of reactive minerals—including olivine, Ca-rich plagioclase, and clinopyroxene—and low content of alteration phases. In the few locations where secondary phases such as serpentine and chlorite were observed, they were confined to grain boundaries and microfractures and did not appear to be pervasive throughout the rock. This preservation of primary mineralogy and textures supports the interpretation that these two lithologies are among the most suitable for CO2 mineral storage within the studied rock formations, under geochemical and thermal conditions favorable for mineral carbonation. This work provides the necessary foundation for future and ongoing experimental validation of reactivity and permeability and detailed site-specific investigations.

KEYWORDS

CO₂ sequestration₁, mineral carbonation₂, mafic rocks₃, Sweden₄, BECCS₅, CCM₆

1 Introduction

Since the Industrial Revolution (\sim 1850), the average global surface temperature has increased by \sim 1.45 °C (World Meteorological Organization, 2024), contributing to more frequent extreme weather, glacial retreat, and record temperatures—especially in the past decade. A recent Intergovernmental Panel on Climate Change (IPCC) assessment has underscored that our current trajectory could lead to an overshoot well over the 1.5 °C target, within a few years, unless immediate and strong reductions in greenhouse gas emissions occur (Allen et al., 2018). The IPCC projects that limiting global warming to 1.5 °C require large-scale deployment of carbon dioxide removals (CDR), such as bioenergy with carbon capture and storage (BECCS). BECCS uses biomass (e.g., agricultural or forestry residues) for energy, captures $\rm CO_2$ post-combustion, and stores it underground. By 2050, BECCS could remove 3–15 billion tonnes of $\rm CO_2$ annually, depending on the specific pathway considered (Allen et al., 2018). While technically feasible, large-scale BECCS deployment may threaten biodiversity, water, food security, and Indigenous rights (Deprez et al., 2024). The sustainable potential is estimated at 2.8 billion tonnes per year—insufficient alone, but still a key mitigation

strategy. For a BECCS value chain to be viable at scale, the availability of secure and permanent CO2 storage is essential. One way of permanently sequestering CO₂ is to allow it to react with calcium-rich mafic silicate rocks, such as basalts (Seifritz, 1990). More recent studies into basaltic bedrock have showcased the efficacy of CO2 storage offering a geochemically secure alternative to conventional storage in porous sedimentary sub-seafloor reservoirs (Oelker et al., 2008; Kelemen and Matter, 2008; McGrail et al., 2017). In basalts and other similar mafic bedrock rich in divalent metal cations, CO2 can be stored through the process of mineral carbonation. When CO₂-buffered water interacts with these rocks, divalent metals such as Ca, Mg, and Fe are released into solution through mineral dissolution. This process increases the pH of the fluid, thereby promoting the precipitation of carbonate minerals such as calcite, magnesite, and ankerite (Matter et al., 2016). A representative example of this reaction is the carbonation of forsterite, eq.

$$Mg_2SiO_4 + 2CO_2 + 2H_2O \rightarrow 2MgCO_3 + H_4SiO_4$$

The Carbfix project began in 2012, near the Hellisheiði geothermal power plant in Iceland, where 230 tonnes of CO₂ were injected into geologically young (Pleistocene-Holocene) basaltic rocks at ~500 m depth (Oelker et al., 2008). By dissolving CO₂ within groundwater at 25-50 °C, the process enhanced solubility trapping and led to rapid mineralization—over 95% within 2 years (Matter et al., 2016). Carbfix has since 2014 continuously injected CO₂ in the basaltic bedrock reservoir. Similarly, the Wallula Basalt Pilot in the US injected ~1,000 tonnes of supercritical CO2 into the Columbia River Basalt (Miocene in age) in 2013. Post-injection analysis revealed mineralization in basaltic breccia, indicated by isotopically distinct ankerite nodules (McGrail et al., 2017). These projects demonstrate that injecting CO2 into reactive basaltic formations can enable efficient and permanent storage via mineral carbonation. Other rock types have also been studied for their potential as CO₂ reservoirs via mineral carbonation. Ultramafic rocks, for example peridotite, have been highlighted by Kelemen and Matter (2008) as promising candidates. A notable recent development is the results from the Project Chalk pilot in Oman, where captured CO2 was injected into Cretaceous peridotite. Chemical and isotopic analyses indicate fast mineralization, with mass balance suggesting ~88% of the CO₂ was converted to carbonate within 45 days (Matter et al., 2025). The outcomes from CarbFix, Wallula, and Project Chalk have been fundamental in demonstrating the feasibility of in situ carbon mineralization. These projects have provided proof-of-concept for the kinetic behavior and reactivity of CO₂ in geological formations, particularly in geologically relatively young, fresh basaltic lithologies. Notably, CarbFix2 extended this understanding to more altered and metamorphosed basaltic phases (Clark et al., 2020), while Project Chalk has shown that injection into low-porosity reservoirs—relying on secondary fracture systems and induced permeability—can still be viable. These findings raise the question to what extent similar approaches may be transferable to geologically older (Proterozoic), less porous rock types that are more widespread globally. Because despite these advances, significant knowledge gaps remain in our understanding-particularly regarding the effectiveness of CO2 mineralization in older, altered, and deformed basalts, as well as in common mafic plutonic and subvolcanic rocks. Formations like these can exhibit variable hydrothermal alteration, metamorphic overprinting, and heterogeneous grainsize distribution, which can affect porosity, permeability, and fluid accessibility. Slower reaction kinetics could be associated with coarse-grained and crystalline lithologies, which may further limit mineralization rates and efficiency. Consequently, the long-term storage potential of these older rock types remains poorly constrained, highlighting the need for experimental and field-based studies to assess their suitability for permanent CO_2 sequestration.

In countries like Sweden, the bedrock lacks extensive fresh basaltic or ultramafic formations, yet it comprises a multitude of variably metamorphosed magmatic rocks with mafic compositions that may still hold potential for CO₂ storage under the right conditions. However, the reactivity, capacity, and long-term stability of formations like this remain largely unexplored. As global CO₂ storage capacity becomes an increasingly critical factor, it is essential to broaden our scope and evaluate subsurface potential wherever geological conditions may be favorable. This begins with detailed investigations of outcrops and bedrock characteristics to identify viable and sustainable storage options.

In this study, we investigate the geological potential for CO_2 storage in the vicinity of major CO_2 point emitters such as the paper and pulp industry through a systematic reconnaissance-style study of mafic rocks throughout Sweden (23 sites; Figure 1). The aim is to identify rock formations theoretically suitable as reservoirs for in-situ mineral carbonation close to emitters (to reduce transport costs for the overall CCS value chain). The geologically descriptive findings of this study lay the foundation for currently ongoing analyses of reactivity, microporosity, permeability, and geochemical fluid flow modeling.

2 Materials and methods

2.1 Mapping, sampling and sample preparation

Fieldwork for this study was conducted across three separate sampling and mapping campaigns. The selection of localities and rock formations was strategized from several factors: proximity to major paper and pulp plants (Figure 1), and existing geological information (databases, maps) from the Geological Survey of Sweden and previous studies. The aim was to ensure a diverse representation of mafic rock types, encompassing both volcanic and plutonic formations, with a preference for formations displaying a relatively limited alteration. To some extent, consideration was also given to areas with presumed higher permeability, such as robust fracture zones, as well as to demographic factors (land use). Because no drill cores are available, all samples were taken from outcrops, carefully avoiding heavily weathered surfaces. To get an understanding of the subsurface conditions in the different study areas, vertical cross sections (based on geophysics) in the SGU maps, together with the size of the surface expressions of the selected lithologies were qualitatively evaluated, so that reasonably large geological units were selected. Within the constraints of field access and visibility, the sample sites were distributed as evenly as possible across the formations. Interpreting exact sample locations within basaltic

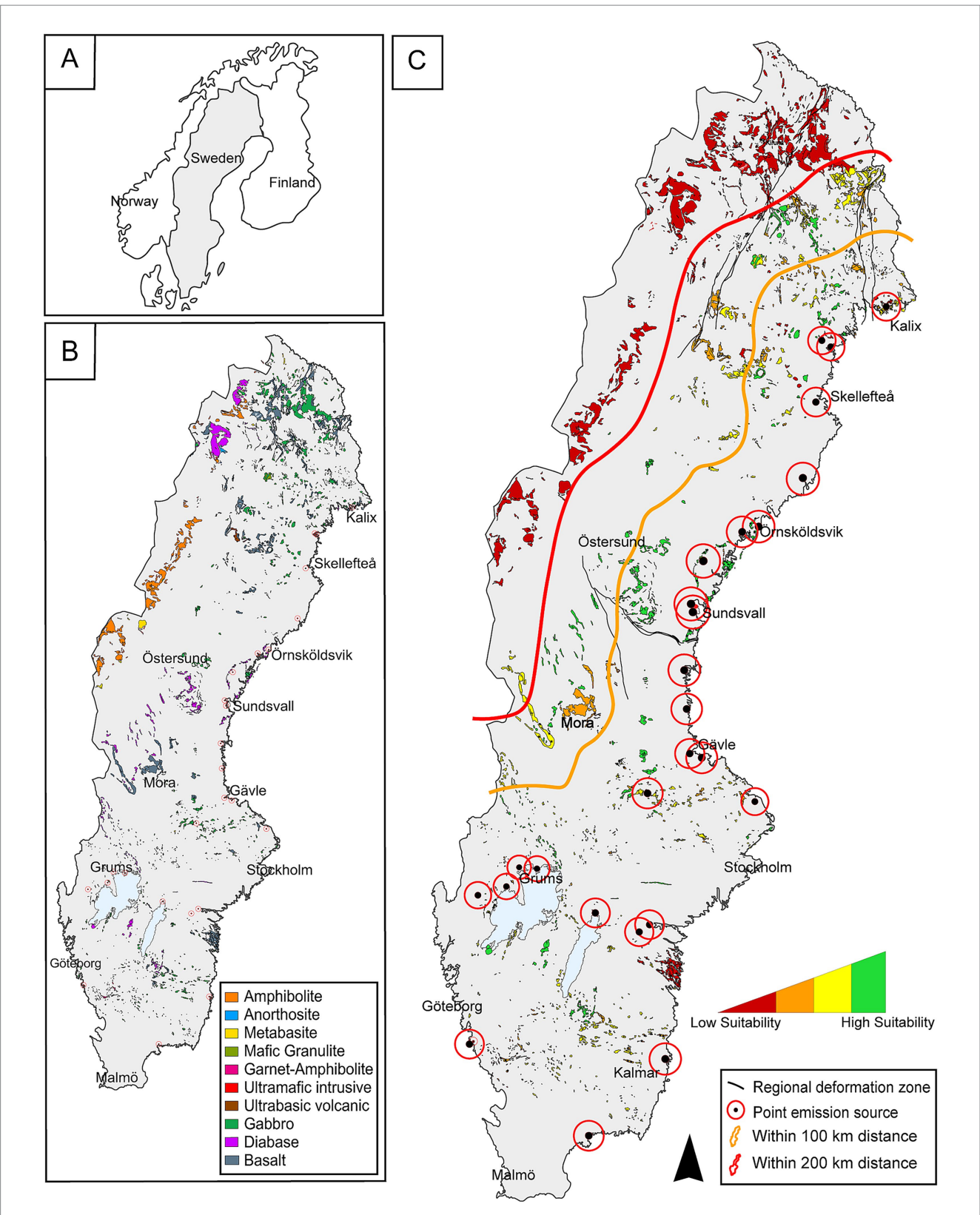
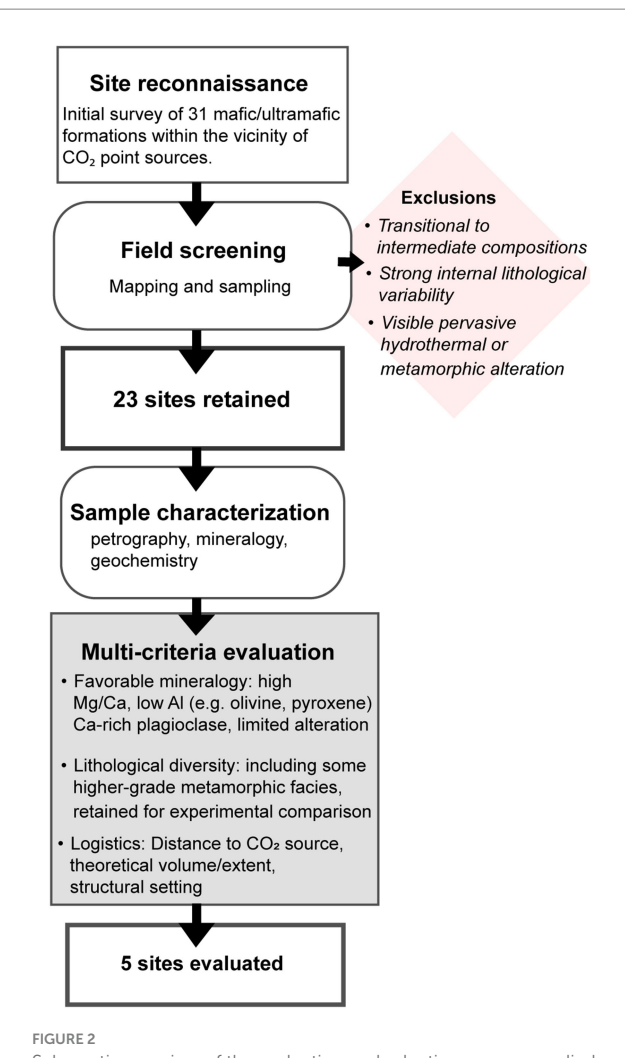


FIGURE 1
Overview maps of Sweden illustrating key parameters used in site selection for geological assessments. (a) Sweden delineated on an overview map of the Nordic countries. (b) Distribution of different mafic rock types across Sweden based on data from SGU (Geological Survey of Sweden) (2013). (c) Suitability map of mafic rock formations, assessed using geological and geochemical criteria (from previous studies and mapping), and further refined with data from fieldwork and analysis. Areas outside the 200 km buffer zone are shown in red to indicate exclusion based on distance from emission sources, rather than geological unsuitability.

stratigraphies and layered intrusions are, consequently, challenging and are here based on dominant mineralogy in relation to classic layered intrusions.

In each fieldwork area, rock formations that in theory would be suitable for CO₂ mineralization (mafic to ultramafic rocks) were sampled. In total, 31 localities were visited for reconnaissance mapping and screening, and samples were taken from 23 of these sites for subsequent analysis. The complete workflow for site evaluation and selection is summarized in Figure 2. Whole-rock geochemical analyses were conducted at both MSALABS and ALS due to time constraints. Comparable analytical methods were employed at both laboratories, including Aqua Regia and four-acid digestions for trace element analysis, and lithium borate fusion for whole-rock and REE determinations. The main procedural difference was that major element oxides were quantified by ICP-ES at MSALABS, whereas XRF was used for these determinations at ALS to facilitate comparison with standard datasets. Quality assurance and control measures included the analysis of replicates and laboratory standards alongside the samples.



Schematic overview of the evaluation and selection process applied to the initial reconnaissance (31 formations) to the final selection of the five case studies.

2.2 Analytical sample characterization

Thin sections were prepared by Precision Petrographics Ltd. (Langley, Canada) from multiple samples collected across the 23 sites. These sections were analyzed for mineralogy and textural features using optical microscopy (Nikon ECLIPSE E600 POL, Zeiss Axioscope 7), under both transmitted and reflected light, at Luleå University of Technology. Furthermore, the samples (incl. Cut-offs) were analyzed using a Scanning Electron Microscope (SEM) and micro-XRF. The SEM (Zeiss Merlin FEG-SEM-EDS/WDS, at LUMIA - Luleå Material Imaging and Analysis), was operated at an acceleration voltage of 20 kV and a probe current of 1 nA, with data processing through the Oxford AZtec software. Micro-XRF analysis was conducted on the cut-offs from thin section preparation using a Bruker M4 Tornado Plus at a resolution of 50 μm, with a time per pixel set to 10 ms. The rhodium tube voltage was set to 50 kV, and the current to 500 µA. Following thorough investigation of mineralogy, chemistry, and petrology from all geological formations, five sites were deemed particularly interesting and were selected for further investigations, based on the multi-criteria evaluation in Figure 2. The estimated modal mineral percentages for the samples studied are presented in Table 1. It should be noted that some samples differed significantly in composition. For example, sample KMv includes both tuffites and more crystalline basalts, with tuffite being by far the most common lithology (Figure 3b). There were also minor variations in the degree of alteration among the samples. Consequently, the modal mineralogy presented here is based on the

TABLE 1 Summary of mineral assemblages and their modal proportions in the studied thin sections, based on petrographic observations and point counting.

	KMvª	ÖMb ^b	NGb ^c	SDold	KGb ^e			
Minerals	Vol%							
Plag	5–16	48-52	50-58	45-50	30-40			
Срх	-	0-3	6–12	20-25	15-20			
Opx	-	-	12-16	-	-			
Ol	-	-	6–15	12-18	-			
Amp	35-45	-	-	1-2	12-16			
Bt	-	-	2-5	2-3	2-4			
Ер		8-10						
Ор	2-7	1-4	1-4	2-4	2-6			
Ap	-	-	Trace	Trace	Trace			
Cal	1-2	1-2	-	-	-			
Qrz	3–11	0-2	-	-	-			
Chl	20-30	8-14	2-3	1-2	15-25			
Pre/Pum	-	10-16	-	-	-			
Other	Other 2–7		2-3	2–5				

^aKalix metavolcanics.

Mineral abbreviations: Plag, plagioclase; Cpx, clinopyroxene; Opx, orthopyroxene; Ol, olivine; Amp, amphibole; Bt, biotite; Ep, epidote; Op, opaque facies; Ap, apatite; Cal, calcite; Qrz, quartz; Chl, chlorite; Pre, prehnite; Pum, pumpellyite.

^bÖje metabasalt.

^cNordingrå gabbro.

^dSundsvall dolerite.

eKallax gabbro

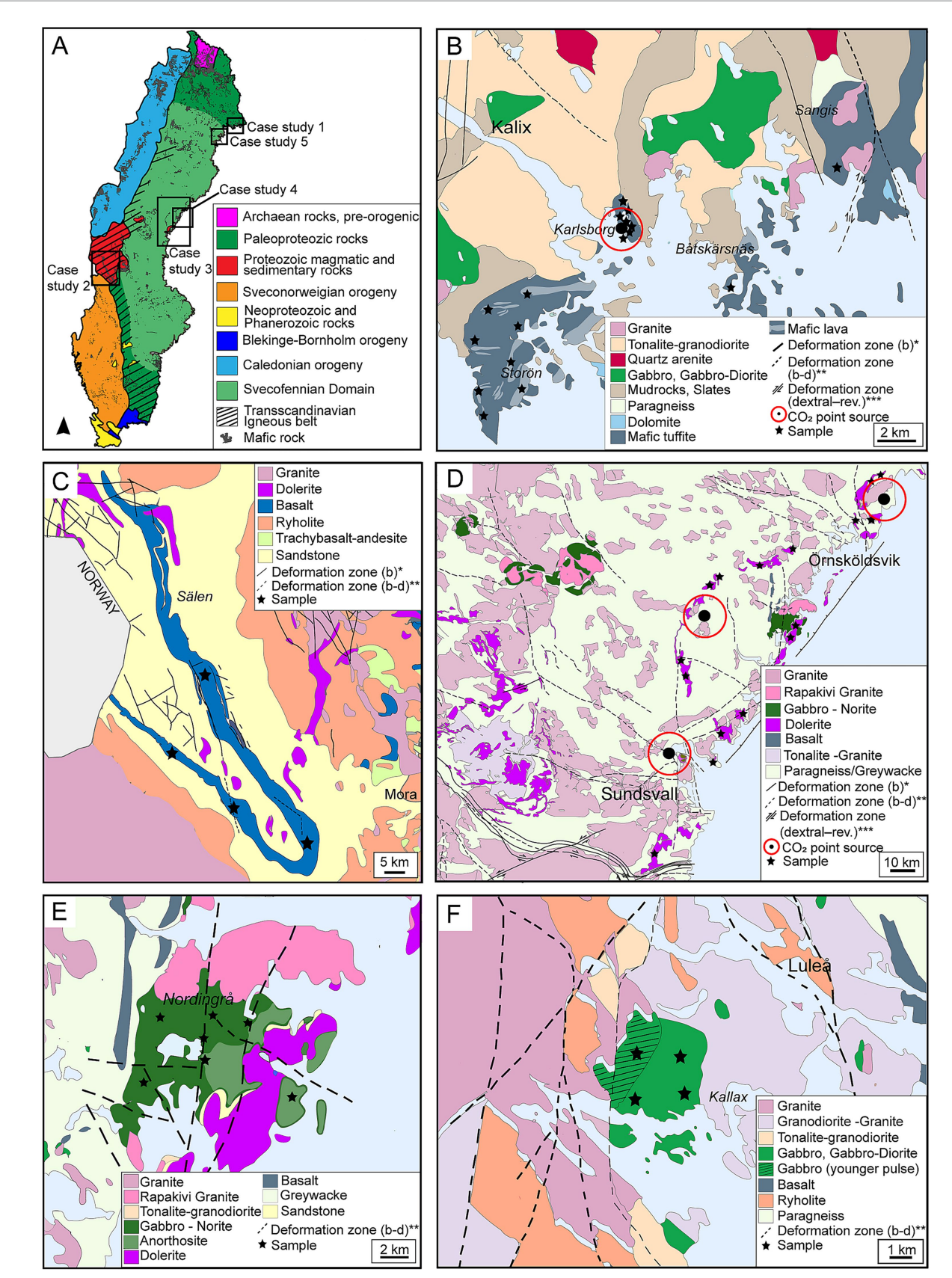


FIGURE 3

Overview and geological context of the five selected case study areas in Sweden, based on data from SGU (Geological Survey of Sweden) (2013), Åhman and Wikström (1990) and Lundqvist (1987). (a) Map of Sweden showing the major lithotectonic units and the locations of the five case study areas. (b) Geological map of the Kalix area (case study 1). (c) Geological map of west-central Sweden, showing the Öje basalt formation (case study 2).

(Continued)

FIGURE 3 (Continued)

(d) Geological map of east-central Sweden covering the Örnsköldsvik–Sundsvall area and the dolerite belt (case study 3). (e) Geological map of the Nordingrå area showing gabbro anorthosite formations (case study 4). (f) Geological map of the Luleå area and the Kallax gabbro (case study 5). *b = brittle, **b-d = brittle-ductile, ***dextral-reverse.

most representative samples from each formation. Outliers that differed markedly in composition were excluded from the modal calculations.

The values were derived primarily from detailed petrographic observations using point counting (~1,000 points/sample), which allowed for more accurate assessment of both primary mineral phases and secondary alteration products. While X-ray diffraction (XRD) analysis was also conducted (PANanalytical Empyrean X-ray diffractometer, at Luleå University of Technology) to support lithofacies identification and confirm mineral presence, it was not used as the primary tool for modal quantification.

3 Geological background

Sweden's bedrock is broadly divided into different major lithological units (Figure 3a). This study investigates localities of mafic rocks within the Svecofennian Domain, as well as associated post-Svecokarelian, Proterozoic units. The Svecofennian Domain (ca. 2.0-1.8 Ga, Stephens, 2020) is primarily composed of Paleoproterozoic metavolcanic and metasedimentary rocks, including amphibolites, gneisses, and greenstone belts, which have predominantly undergone metamorphism under amphibolite facies conditions, with localized occurrences of greenschist and granulite facies. In contrast, the post-Svecokarelian rocks include dolerite, clastic sedimentary rocks, basalt, and intrusives such as granite, syenites, gabbro, and anorthosite. These units span from approximately 1.7 to 0.95 Ga (Stephens, 2020) and are related to episodes of intracratonic rifting. These rocks, found in west-central Sweden and the inland areas of central Sweden, exhibit varying degrees of metamorphism due to differences in their tectonic setting and timing of formation, but generally display lower metamorphic grades than rocks within the Svecofennian Domain.

4 Results

4.1 Assessing and selecting suitable localities

During selection of study areas, suitable lithologies close to industry CO_2 point emitters were prioritized over possibly better suited lithologies situated far from emitters or infrastructure since poor transportation networks make these sites unlikely candidates for storage (Figure 3). From mapping, sampling and mineralogical characterization of 23 sites throughout Sweden, five were selected for further assessment (Figure 3): (1) Kalix metavolcanic units (KMv), (2) Öje basalt (ÖMb), (3) Nordingrå gabbro (NGb), (4) Örnsköldsvik-Sundsvall dolerite (SDol), (5) Kallax gabbro (KGb).

4.2 Petrography, mineral chemistry and field observations

4.2.1 Metavolcanic rocks (Kalix, Öje)

Kalix Metavolcanics: The metavolcanic rocks around Kalix (Figure 3b) are dominated by gray to dark gray, tuffitic volcanoclastic rocks. This rock type typically displays layering (Figure 4b), which in thin section corresponds to compositional laminae 1-10 mm thick (Figure 5d), composed of alternating bands of quartz, iron oxides, mica, hornblende, and plagioclase (oligoclase)—the latter commonly altered to sericite and occasionally scapolite. The matrix is finegrained, with typical grain sizes between 100 and 300 μm . Interbedded horizontal carbonate layers occur in several outcrops, and quartzcalcite veins (0.1-1 mm wide) are widespread. Disseminated pyrite (100–200 μm grain size) are often accompanied by minor chalcopyrite. A quartz content of ~10 vol% in several samples suggests significant siliciclastic input, and quartz-feldspar aggregates point to a source from previously lithified volcaniclastic material. Overlying the volcanoclastic rocks of the Karlsborg Formation are slates from the Råneå Group, which locally resemble the tuffites in appearance. On Storön, most sampled outcrops consist of tuffitic rocks similar to those elsewhere in the area. However, several exposures feature medium- to coarse-grained lithologies with distinct textures and appearances (Figure 5e). These units are interpreted as subvolcanic intrusions or lava flows genetically related to the surrounding volcaniclastic sequence. They lack typical basaltic features such as vesicles, phenocrysts, or preserved flow structures, and original volcanic textures have been obliterated by recrystallization and deformation. These coarser rocks are generally massive and do not exhibit the fine compositional layering seen in the tuffites. Despite their textural differences, both the tuffitic and coarser volcanic/subvolcanic rocks share a similar metamorphic mineral assemblage. Amphibole, primarily hornblende, is dominant (>35 vol%; Table 2), often forming acicular or radiating grains with strong preferred orientation. Plagioclase, quartz, and biotite are also present, along with common oxide minerals such as magnetite and ilmenite. Trace phases include titanite and zircon, typically concentrated in oxide-rich zones. The overall observation indicates that the rocks are within amphibolite facies.

 \ddot{O} je basalt: The second metavolcanic formation studied is located in western Sweden near the Norwegian border (Figure 3c). The \ddot{O} je basalt, which exhibits a synformal structure, is interbedded within Jotnian sandstone. Mapping and sampling were focused on the southern exposures of the basaltic unit. While previous studies (e.g., Ripa and Mellqvist, 2012) have documented features such as tuffaceous components and pillow basalts in other areas, the sections examined in this study are relatively uniform, consisting predominantly of massive, fine-grained basalt (100–300 μm). This basalt typically forms subhorizontal, aphanitic layers within the sandstone and is dark gray to reddish-brown, equigranular, and intergranular in texture. It is composed of randomly oriented albitic



FIGURE 4
Field images. (a) bedrock exposure in the Nordingrå gabbro complex. (b) tuffite in Kalix showing clear compositional lamination. (c) internal layering divided by thin carbonate veins in one of the samples sites in Öje. (d) plagioclase crystals from an anorthite exposure in Nordingrå. (e) insulated coarser grained dolerite dyke within a dolerite close to Örnsköldsvik.

plagioclase laths (>48 vol%; Table 1) and interstitial mafic mineral phases (Figures 5a-c). Clinopyroxene, the primary mafic mineral, is extensively altered or replaced by chlorite. Accessory phases include titanomagnetite, magnetite, ilmenite, granular quartz, and trace pyrite. Local variations occur in the eastern part of the study area, where porphyritic textures develop with plagioclase phenocrysts in a finer-grained groundmass (Figure 5b). Some exposures also feature subparallel, sheet-like units resembling sedimentary bedding, separated by thin, laterally continuous carbonate-rich horizons (Figure 4c). Amygdaloidal textures are present in several outcrops, with amygdules infilled by chlorite, quartz, calcite, and occasionally chalcedony and pumpellyite. Secondary alteration minerals—pumpellyite, epidote, and prehnite—occur in both matrix and veins (Figure 5f). Crosscutting magnetite-rich veins encapsulate quartz and contain inclusions of zeolite minerals and chlorite. Isolated cubic halite crystals were also identified. The co-occurrence of prehnite, pumpellyite, and halite

indicates low-grade regional metamorphism within the prehnitepumpellyite facies.

4.2.2 Plutonic rocks (Nordingrå, Sundsvall, Kallax)

Dolerites Örnsköldsvik and Sundsvall: Mafic intrusions belonging to the Central Scandinavian Dolerite Group (CSDG) were studied in eastern Sweden, north-northeast of Örnsköldsvik and northeast of Sundsvall (Figure 3d). In the Husum and Örnsköldsvik areas, the dolerites are medium- to coarse-grained, with a slight increase in grain size toward the centers of the intrusions. The rocks are gray to dark gray and exhibit well-developed ophitic to subophitic textures (Figure 4e). These textures are defined by abundant, tabular plagioclase crystals (predominantly labradorite, ~45–50 vol%) enclosed by interstitial mafic mineral phases, forming a holocrystalline fabric (Figures 6c, f). The mafic component is dominated by ferroan augite (20–25 vol%), with olivine (Fo64 12–18 vol%) occurring as subhedral to anhedral phenocrysts (Figure 6e). Olivine is variably altered, with

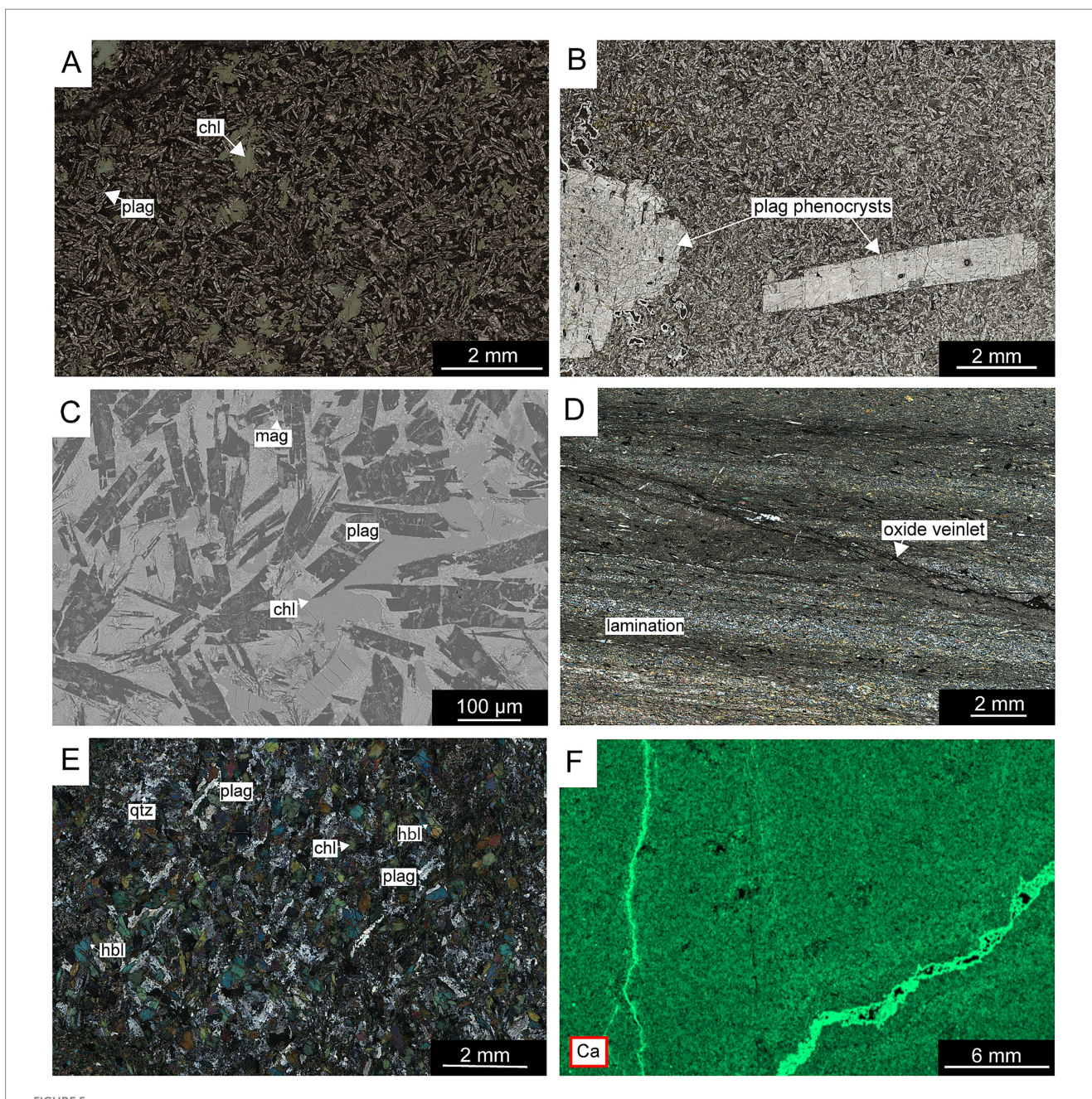


FIGURE 5
Photomicrographs (plane-polarized light, cross-polarized light), μXRF scan and backscattered electron (BSE) image of metavolcanic rocks from Öje and Kalix. (a) Overview of albite-rich Öje metabasalt. (b) Plagioclase phenocrysts (>2 mm) in a fine-grained basaltic matrix in the Öje basalt. (c) BSE image showing randomly oriented plagioclase laths with altered mafic phases infilling interstitial spaces in the Öje basalt. (d) Laminated tuffite from Kalix. (e) Overview of the minerology of the basaltic unit in Kalix. (f) μXRF scan elemental map showing Ca-distribution in the Öje metavolcanic rock.

TABLE 2 Bulk chemical composition given as weight percentages.

Sample	SiO ₂	Al ₂ O ₃	Fe ₂ O ₃	MgO	CaO	Na₂O	K ₂ O	TiO ₂	MnO	P ₂ O ₅	Cr ₂ O ₃	LOI
KMvª	49.11	14.26	14.15	7.31	9.63	3.36	0.29	1.00	0.22	0.07	0.03	0.65
ÖM ^b	46.89	15.74	14.36	5.12	8.94	2.43	0.14	1.90	0.21	0.32	0.01	4.21
NGb ^c	45.54	15.08	19.24	8.95	7.89	2.21	0.64	0.63	0.21	0.18	0.01	-0.48
SDol ^d	44.73	14.12	16.36	11.55	8.37	2.27	0.50	1.62	0.22	0.18	0.01	0.32
KGb ^e	45.82	15.35	12.35	8.11	12.95	2.29	0.21	1.79	0.16	0.51	0.02	0.20

^aKalix metavolcanics.

^bÖje metabasalt.

[°]Nordingrå gabbro.

^dSundsvall dolerite.

eKallax gabbro.

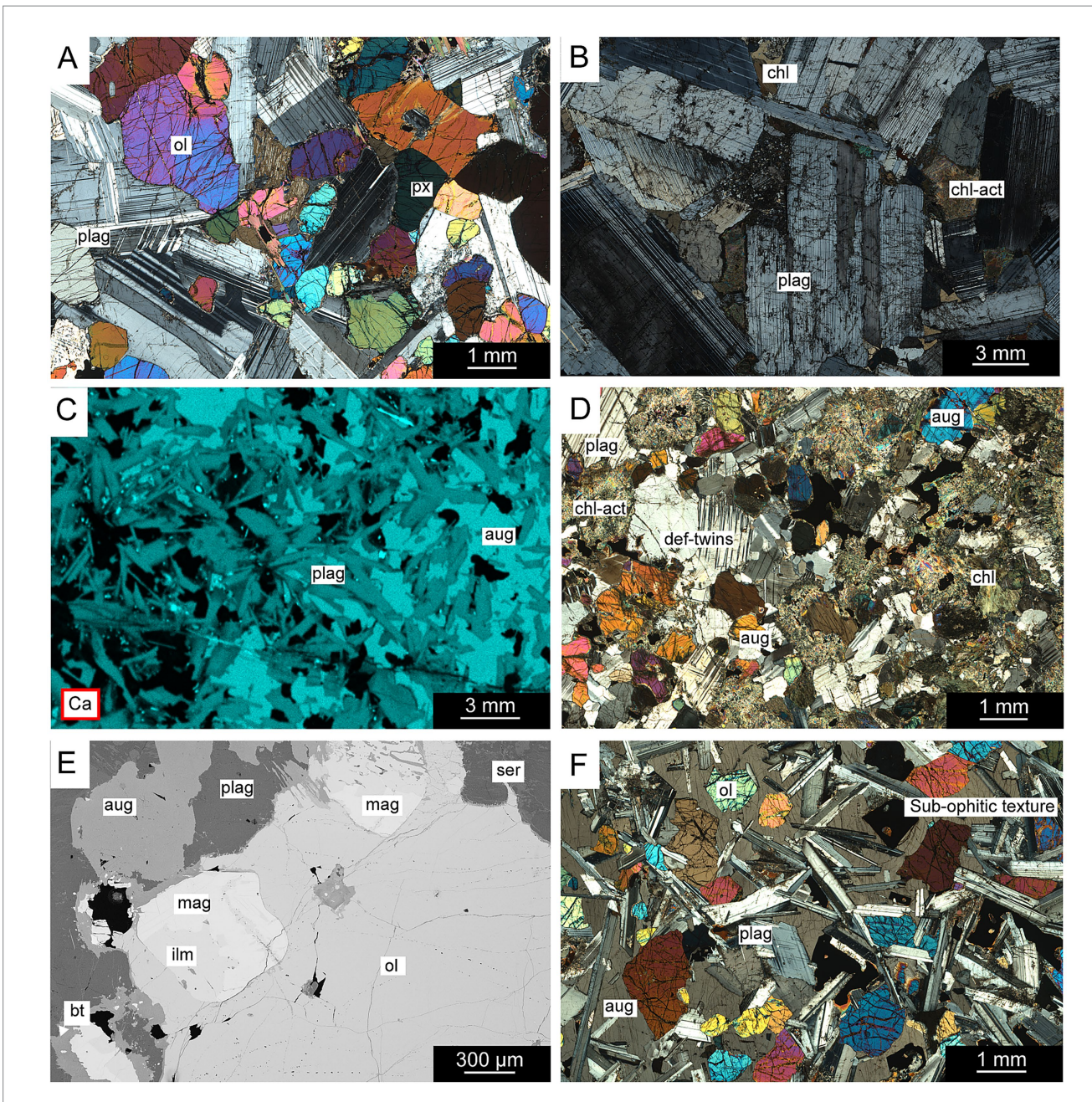


FIGURE 6
Photomicrographs (plane-polarized light, cross-polarized light), μXRF scan, and backscattered electron (BSE) image of the plutonic rocks in Nordingrå, Örnsköldsvik, Sundsvall and Kalix. (a) Olivine and pyroxene crystals set in a plagioclase-rich matrix in the Nordingrå plutonic rock. (b) Coarse plagioclase grains within anorthosite from Nordingrå. (c) μXRF elemental map showing calcium distribution in a CSDG dolerite sample from Örnsköldsvik. (d) Overview of the mineralogy in the Kallax gabbro. (e) BSE image showing an overview of the mineralogy in a CSDG sample from south of Örnsköldsvik. (f) Subophitic texture in dolerite from the CSDG, south of Sundsvall.

minor serpentinization along fractures and grain boundaries, often accompanied by fine-grained magnetite and chlorite-filled microfractures. Accessory minerals include Fe-Ti oxides (magnetite and ilmenite), biotite (commonly associated with oxides), apatite, ulvöspinel, and minor sulfides such as pyrite, chalcopyrite, and pyrrhotite. Jointing is common at the margins of the dykes, and calcite is occasionally present on joint surfaces. At the northernmost locality, the dolerite displays a lighter gray to greenish color, and although ophitic textures are still recognizable, they are more subdued due to alteration. This locality is marked by extensive chloritization and,

unlike the majority of the sampled dolerites, shows signs of low-grade metamorphic overprinting. Prehnite-pumpellyite assemblages in vein networks indicate localized low-grade metamorphism. Despite this exception, the dolerites across the broader study area are consistently classified as olivine dolerites based on their primary mineralogy.

Nordingrå gabbro: In the same region, the Nordingrå granite-gabbro complex was also investigated (Figure 3e). Granite dominates the northern part of the complex, while gabbro, leucogabbro, and anorthosite occur mainly in the south. This study focused on the gabbro and anorthosite units, which exhibit a close genetic

relationship, marked by irregular contacts—particularly between leucogabbro and anorthosite—and gabbroic dykes intruding the anorthosite. Gabbro is most common in the western part of the massif, whereas leucogabbro and anorthosite are predominantly exposed in the east. The gabbro is typically dark gray, massive, and medium- to coarse-grained, with a holocrystalline, equigranular texture (Figure 4a). In thin section, the gabbro displays a phaneritic to locally poikilitic fabric, composed primarily of plagioclase (labradorite to andesine, 50-58 vol%) and a mafic assemblage of orthopyroxene and clinopyroxene (~22 vol%). Olivine (up to 15 vol%) occurs as subhedral to anhedral grains, typically interstitial to plagioclase and pyroxene, with grain sizes ranging from 0.5 to 2 mm (Figure 6a). In some samples, large pyroxene grains enclose smaller plagioclase laths, forming poikilitic textures. Orthopyroxene grains commonly contain exsolution lamellae of clinopyroxene, and vice versa, indicating slow cooling and subsolidus re-equilibration. The clinopyroxene composition is En₄₅-Fs₁₀-Wo₄₅, while orthopyroxene is En₆₀-Fs₄₀. The opaque mineral assemblage includes magnetite and ilmenite, with minor pyrrhotite and chalcopyrite. Accessory minerals such as biotite, apatite, chlorite, actinolite, magnesio-anthophyllite, and prehnite are present, particularly in the more altered samples. Serpentinization is common along fractures in olivine and at grain boundaries, often accompanied by fine-grained magnetite. Local chloritization and replacement of mafic phases by magnesio-anthophyllite indicate a low-grade metamorphic overprint, likely reaching sub-greenschist facies conditions. The anorthosite is lighter in color and coarsegrained, with Ca-rich plagioclase forming grains up to 3.5 cm in size (Figures 4d, 6b). These plagioclase crystals often display welldeveloped twin lamellae, though deformation and extensive sericitization have locally altered their original structure. Anorthosite frequently occurs as enclaves within the leucogabbro, and both units show a higher degree of metamorphic alteration compared to the gabbro. Accessory minerals in these rocks include amphibole, biotite, apatite, epidote, actinolite, and chlorite, with localized feather-like prehnite replacing primary phases. Oxides are dominated by ilmenite and magnetite. The Nordingrå complex shows no evidence of deformation related to later tectonic events, such as those associated with the adjacent Central Scandinavian Dolerite Group (CSDG) intrusions, preserving its original intrusive relationships and magmatic textures. Kallax Gabbro: The third plutonic rock type investigated in this study is the Kallax gabbro (Figure 3f). This gabbroic intrusion is interpreted to consist of two magmatic pulses, dated to approximately 1.9 and 1.8 Ga, with the distribution of the younger phase delineated through geophysical data (Wikström and Söderman, 2000). However, field mapping did not reveal a distinct contact between the two units. The intrusion is largely massive and medium-grained, with some outcrops of the older gabbro displaying subtle layering in the form of alternating dark gray and light gray bands. Fine-grained mafic dykes are present in both the older and younger gabbro units. The gabbro exhibits a holocrystalline texture, with grain sizes ranging from 1 to 2.5 mm. The igneous fabric is generally well preserved, although secondary mineral replacement is locally pervasive, particularly along grain boundaries and fractures (Figure 6d). The primary mineral assemblage consists of plagioclase (labradorite), augite, magnetite, and ilmenite. Plagioclase content varies between 30 and 45 vol%, and in more altered samples, it is partially to completely replaced by sericite, especially along cleavage planes and fractures. Augite, typically subhedral to anhedral and ranging from 0.5 to 2 mm in size, contributes approximately 15–20 vol% of the rock. In altered domains, augite is progressively replaced by chlorite, actinolite, epidote, and biotite, with interstitial grains often exhibiting actinolite-rich reaction rims indicative of metasomatic alteration. These secondary phases—particularly chlorite and actinolite—are widespread, and in more intensely altered samples, biotite becomes a prominent replacement product. Accessory minerals include apatite and minor sulfides, primarily pyrite. These mineralogical transformations, along with the development of chlorite- and magnetite-filled microfractures and the replacement of augite and plagioclase, reflect metamorphism within the greenschist to lower amphibolite facies.

4.3 Geochemistry

The bulk chemical composition data for the whole-rock samples are presented in Table 2. Classifying metamorphosed volcanic rocks using the Total Alkali-Silica (TAS) diagram is inherently challenging, as major elements often become mobile during metamorphism and alteration. In particular, potassium (K) and sodium (Na) are highly susceptible to mobilization under these conditions, which can significantly alter the rock's original geochemical signature and result in misclassification on a TAS diagram. To address this issue, the data were plotted on the igneous spectrum diagram proposed by Hughes (1973) (Supplementary Figure S1). Most of the metavolcanic rock samples from Kalix exhibit evidence of Na-metasomatic alteration, whereas the samples from Öje largely fall within the igneous spectrum, with the exception of a single outlier (Supplementary Figure S1). To classify the volcanic rocks, we therefore employed immobile element ratios and plotted the data on a Zr/Ti vs. Nb/Y diagram following Pearce (1996), based on Winchester and Floyd (1977) (Figure 7a). The majority of the samples cluster tightly within the sub-alkaline basalt field, indicating a predominantly tholeitic to calc-alkaline magma series—characteristic of a volcanic arc or back-arc tectonic setting. Two metavolcanic samples from Kalix display slightly elevated Nb concentrations, thus plotting within the alkali basalt field. These outliers may reflect subtle variations in source composition or localized enrichment in alkalis due to secondary alteration. Plutonic samples were likewise assessed for alteration using the igneous spectrum diagram of Hughes (1973), where all data points fall between the Na- and K-metasomatic alteration trends, indicating minimal metasomatic overprint (Supplementary Figure S1). Given the limited extent of alteration, the samples were subsequently classified using the TAS diagram proposed by Middlemost (1994) for plutonic rocks (Figure 7b). The gabbro from Kallax, along with those from the Nordingrå massif, plots near the boundary between the gabbro and alkalic gabbro fields. This positioning suggests transitional compositions that may reflect low to moderate alkali enrichment, potentially linked to source variability or minor metasomatic overprint. In contrast, the majority of dolerite samples from Sundsvall and Örnsköldsvik are tightly clustered within the alkalic gabbro field, indicating a relatively uniform and mildly alkaline composition. Four dolerite samples, however, deviate from this main cluster, trending toward the monzogabbro/foid gabbro field.

Alteration indices (Chemical Index of Alteration, CIA, and Mafic Index of Alteration, MIA) were calculated for each formation (Babechuk et al., 2014). These data are available in the appendix

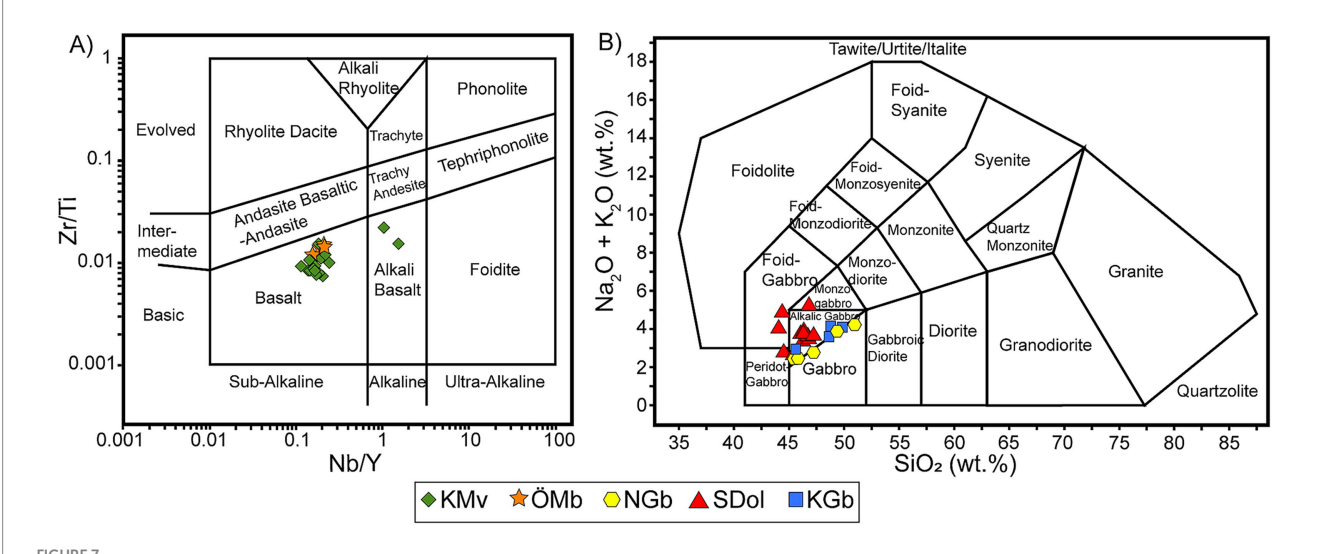


FIGURE 7
Classification diagrams based on whole rock geochemical data (a) Zr/Ti vs. Nb/Y diagram proposed by Pearce (1996), based on Winchester and Floyd (1977). (b) Classification and nomenclature of the plutonic rocks based on the total alkalis ($Na_2O + K_2O$) versus SiO_2 (TAS) diagram proposed by Middlemost (1994).

(Supplementary Table S2). Both the dolerites from Sundsvall and Örnsköldsvik and the Nordingrå gabbro show minor leaching (Δ MIA(R) > 0 with moderate CIA*), whereas the Kallax gabbro – although more altered mineralogically – shows a low/flat MIA(R). This could reflect retention/addition of Mg (\pm Fe) in secondary phases under oxidizing conditions, which decouples MIA from CIA during alteration. The Öje basalt (prehnite–pumpellyite to lower greenschist) shows near-fresh values, indicating only minor leaching with Fe largely retained. For the metavolcanics in Kalix, metamorphic overprint, and strong deformation obscure the protolith, so the indices are heterogeneous and not straightforward to interpret in terms of primary weathering intensity.

5 Discussion

The mineral carbonation process in mafic and ultramafic rocks involves the binding of injected CO₂ (supercritical or dissolved) with divalent metal cations leached from the bedrock reservoir to form carbonates (Oelkers et al., 2008). For this to work, it is crucial to understand the primary mineralogy of the storage reservoir, as it will constrain the efficiency of mineral carbonation reactions. In addition, it is important to estimate whether the porosity and permeability are sufficient for fluid injection and migration. In many crystalline settings, the expected primary porosity of older plutonic rocks is close to zero, intergranular porosity may vary but is generally low (<2%; e.g., Möri et al., 2021). Similarly, in metamorphosed basaltic formations, vesicular porosity is usually destroyed or sealed by secondary minerals (Neuhoff et al., 1999). Consequently, flow and storage in such reservoirs would be fractured-controlled, similar to what is anticipated for peridotite-hosted reservoirs such as in the Project Chalk pilot in Oman, where Matter et al. (2025) reported porosity decreasing from ~16% near the surface to <1% at depth. If there is insufficient primary porosity in the reservoir, techniques such as hydroshearing (not to be confused with hydrofracking where environmentally deleterious chemicals typically are used to extract fossil fuels) may be used to generate secondary porosity through deep-drilling and injection of water into the subsurface. This technique, used in Enhanced Geothermal Systems (EGS), may provide enough pore space to allow injection of a CO₂-rich fluid and subsequent mineral carbonation of the CO₂, forming secondary carbonate minerals in the reservoir, at depth in the crust. As the porosity and permeability properties are critical for successful storage, x-ray tomographic analysis coupled with fluid flow modeling is presently being performed on all five case studies. For mineral carbonation to be feasible, however, mineralogy needs to be reactive enough with CO₂. Hence, in the following section, the mineralogy is assessed with respect to theoretical potential for storage of CO₂ in the five selected reservoirs.

5.1 Metavolcanics rocks (Kalix, Öje)

The basaltic rocks in the Kalix area consist of amphibolite facies tuffites with associated lava flows of similar chemistry and mineralogy. Both the tuffite and the more crystalline volcanic sections are predominantly composed of hornblende, implying that the major Ca-bearing phase in the basalt is hornblende, with a smaller portion of Ca2+ in albite and chlorite. Previous studies have examined the kinetics and suitability of various amphiboles for carbonation. In a study by Heřmanská et al. (2022), hornblende dissolution rates were compared with model-produced dissolution rates, which resulted in rates ranging from $10^{-8.4}$ mol/m²/s at pH 1.6 to $10^{-12.3}$ mol/m²/s at pH 7.0. Experimental studies covering higher temperatures and higher pH levels are few, causing models to diverge at neutral to basic pH. Heřmanská et al. (2022) notes that the presence of aluminum (Al) in the mineral framework appears to cause slower dissolution rates at near neutral pH, since the same dissolution rate trend is not seen in Al-free amphiboles. Hornblende was not considered in the theoretical uptake estimates (Table 3), leaving albite as the main reactive component in the metavolcanic rocks from Kalix. However, the

TABLE 3 Modal abundances (%) of reactive minerals in a representative sample for each rock unit and the resulting theoretical CO₂ uptake values (wt%) based on two methods

Sample	Ol	Срх	Орх	Lab	Alb	Ер	Pre	Act	CO ₂ Uptake (wt%, elemental)*	CO ₂ Uptake (wt%, molar)**	
Modal (%)											
KMv	-	-	-	-	15.2	-	-	-	0.71	2.55	
ÖMb	-	3.01	-	-	50.82	10.23	8.83	-	14.86	12.55	
NGb	12.46	9.02	12.01	58.24	-	-	-	-	20.17	24.23	
SDol	16.48	25.17	-	47.69	-	-	-	-	23.12	27.20	
KGb	-	20.23	-	37.79	-	-	-	12.21	15.33	16.06	

*Calculated using measured elemental compositions (Ca, Mg, Fe) from reactive minerals. Stoichiometric CO₂ conversion factors were applied, and values were weighted by modal mineral abundances. **CO₂ uptake values were calculated based on mineral-specific molar masses and the number of reactive CO₂ molecules per formula unit, then weighted according to each mineral's modal abundance in the sample. The elemental method uses mineral-specific compositions with stoichiometric conversions, while the molar method assumes ideal mineral formulas complete carbonation of end members. See footnotes on calculation details. Presenting both methods allows comparison between composition-specific and theoretical maximum uptake estimates. KMv = Kalix metavolcanics ÖMb=Öje metabasalt NGb= Nordingrå gabbro SDol = Sundsvall dolerite KGb = Kallax gabbro Mineral abbreviation: Ol=olivine, Cpx=clinopyroxene, Opx=orthopyroxene, Lab=labradorite, Alb=albite, Ep=epidote, Pre=prehnite, Act=actinolite.

limited reactivity of albite might be insufficient to facilitate effective mineral carbonation. In the solid-solution series of plagioclase feldspars, most of the plagioclase in the samples from the Kalix rocks fall within the range of oligoclase to albite. Studies investigating the dissolution rates of plagioclase (e.g., Gudbrandsson et al., 2014) have shown that the Ca-rich endmember, anorthite, dissolves up to 10 times faster than the Na-rich endmember, albite, under acidic conditions (pH < 4), while the difference between endmembers becomes negligible at more alkaline conditions. Albite contains less Al in its tetrahedral framework, resulting in fewer Al-O bonds available for proton attack (Gudbrandsson et al., 2014). During dissolution, it readily forms a stable, Si-rich surface layer dominated by strong Si-O-Si bonds, which are more resistant to breakage than the Al-O bonds in anorthite. This layer acts as a kinetic barrier, slowing further albite dissolution (Oelkers et al., 1994). Given the mineralogy of the Kalix metavolcanics, this reservoir is likely unsuitable for CO2 storage through mineral carbonation due to the limited reactivity of their primary mineral components.

The Öje basaltic rock unit (Figure 3c) is less affected by metamorphism and occurs interlayered with sandstone, forming basaltic lava flows (~300 m thick) between sequences of sandstone. The Öje basalt has undergone prehnite-pumpellyite metamorphism and predominantly consists of plagioclase (albite to oligoclase), chlorite, epidote, prehnite, and pumpellyite. Only a small portion of the original clinopyroxene remains (< 3 vol%, Table 1). With respect to theoretical reactivity, these minerals, combined with a higher proportion of plagioclase, are supposedly more advantageous than those comprising the metavolcanic rocks in Kalix. Although the basalts from Öje are less metamorphosed compared to the Kalix metavolcanic rocks, they are still significantly altered regarding primary mineralogy which negatively impacts the CO₂ reactivity. Experimental work generally shows that fresh basalt is more reactive than altered basalt (Marieni and Oelkers, 2018; Clark et al., 2020; Delerce et al., 2023). The main difference in reactivity between fresh and altered basalts is not necessarily due to the presence of glass, as Mesfin et al. (2023) found that Si release rates in labradorite and basaltic glass were almost identical. Instead, the presence of secondary alteration minerals appears to have the greatest impact on the difference in reaction rates between fresh and older altered rocks the most. Minerals like chlorite and clay minerals typically have larger reactive surface areas but slower dissolution rates, often covering or replacing the primary reactive mineralogy (Malmström et al., 1996). On the other hand, some reactive secondary minerals in altered basalts, such as zeolite and epidote, release Ca and Mg and helps neutralize acidic CO2-rich fluids, supporting carbonate formation (Delerce, 2023). Notably, the Öje basalt samples contain a significant amount of secondary minerals, including epidote, with its high Ca/Si ratio, could contribute to the release of Ca, especially under acidic high-temperature conditions (>100 $^{\circ}$ C), thereby aiding in pH neutralization (Marieni et al., 2021). Epidote was included as a reactive mineral contributing to the overall uptake of CO2 in the rocks as presented in Table 3. The contribution of epidote to the overall uptake is however considered small (~0.8) due to low modal amounts. Another mineral in the Öje basalt that contains divalent cations is chlorite. A reactive transport modeling study by Mishra et al. (2023) showed that, although chlorite releases cations that support carbon mineralization, its relatively low reactivity delays dissolution—peaking between 200 and 500 years post-injection—making it more influential in long-term rather than early-stage carbonate formation. Comparison between the Kalix metavolcanics (amphibolite facies) and the Öje metabasalt (prehnite-pumpellyite to lower greenschist facies) highlights notable differences in reactivity related to metamorphic grade. Due to the presence of phases such as epidote, prehnite, and pumpellyite, along with a relatively high plagioclase content—despite its compositional trend toward oligoclase-albite—the Öje metabasalt exhibits higher predicted reactivity compared to the Kalix metavolcanics, which in addition is also characterized by lower plagioclase content and, in some cases, elevated quartz concentrations (~10 vol%). Dissolution rates for minerals in prehnite to greenschist rocks are still sluggish compared to fresh mafic minerals like olivine and pyroxene, which drive the rapid cation release. Thus, while these minerals may contribute to carbonation over longer timescales,proceeding at rates substantially faster than comparable reactions in subseafloor sedimentary reservoirs (e.g., sandstone) - they are not optimal for the fast reactions required for mineral storage in mafic and ultramafic reservoirs.

5.2 Plutonic rocks (Nordingrå, Sundsvall, Kallax)

In the Nordingrå area, granite dominates the surface outcrops. However, gravimetric surveys indicates that this granite forms a ~ 1 km thick sliver above the Nordingrå gabbro which is estimated to be up to to ~6 km thick (Lindh et al., 2001). The Nordingrå gabbroanorthosite complex is a layered mafic intrusion in which fractional crystallization and cumulate sorting produce a systematic vertical stratigraphy. Upper sections in mafic layered intrusions are typically plagioclase-rich with Fe-Ti-oxide/apatite seams, whereas deeper levels commonly grade into more ultramafic cumulates (olivine \pm pyroxene) with higher-An plagioclase. Layering can be cyclic, and reversals from magma replenishment are possible, nevertheless, where only the upper-middle levels are exposed, it is reasonable to infer olivine- and pyroxene-richer assemblages with depth. This architecture makes layered intrusions interesting targets for mineral carbonation. However, to add to the complexity, the degree and style of alteration may vary with permeability and fluid access, so site-specific reactivity cannot be assumed from surface exposures alone. A robust assessment of the whole formation in the future will require subsurface constraints (e.g., targeted geophysics and/or coring).

In contrast to basaltic rocks, plutonic rocks are less commonly considered for in-situ mineral carbonation, likely because the storage would to a large degree have to utilize and rely on secondary porosity, e.g., fault zones and fracture networks. This perception may have resulted in so far limited scientific interest in exploring the potential for mineral carbonation in plutonic rocks. An experimental study on gabbroic anorthosite in Portugal, however, showed promising potential for mineral carbonation (Berrezueta et al., 2023). Torrão-Odivelas Massif (Berrezueta et al., 2023) and the Nordingrå complex are not closely comparable in overall character, but they exhibit some similarities—the layered structure of the gabbros, their genetic association with anorthosites, and the presence of comparable minerals and mineral textures. The gabbroic parts of the Nordingrå complex are dominated by Ca-rich plagioclase (mainly labradorite), with significant amounts of orthopyroxene, although the mineral proportions likely vary with depth due to the layered nature of the gabbro. Clinopyroxene and olivine (modal proportion, ca. 9.02 and 12.5%; Table 3) also contributes to the high theoretical CO₂ uptake (Table 3). Olivine significantly enhances the overall reactivity of a rock assemblage but like other reactive minerals, olivine dissolution rates typically tend to slow down over time due to the formation of a Si-rich passivation layer at the rims of olivine grains, resulting from preferential Mg leaching and/or simultaneous dissolution and Si reprecipitation (Johnson et al., 2014). This passivation layer limits the continued reaction by hindering H⁺ ions from reaching the unreacted mineral surface, and the reaction then becomes dependent on diffusion through this layer (Wang et al., 2019). However, during these mineral reactions, olivine may fracture due to so called reactiondriven cracking (Zhu et al., 2016; Kelemen et al., 2019), exposing fresh reactive mineral surfaces. This process of generating secondary porosity is particularly advantageous in low-porosity rocks, as plutonic rocks would typically be regarded as, where fluid access is limited, and additional space would need to be created for reactive CO2 fluids to migrate and continuously expose fresh mineral surfaces for sustained CO2 uptake.

Furthermore, pyroxene constitutes a significant proportion of the mineralogy in the Nordingrå gabbro-anorthosite complex. Pyroxene has been identified as a reactive mineral suitable for mineral carbonation (e.g., Brantley and Chen, 1995). When pyroxene dissolves, protons from the fluid replace metal cations at the mineral surface, releasing those cations into solution (Oelkers and Schott, 2001). Subsequently, the silica near the removed cations begins to break down slowly. Experimental work by Oelkers and Schott (2001) and Oelkers et al. (2009) has shown that breakdown of the silica framework is the rate-limiting step for pyroxene dissolution, In other words, although cation exchange occurs relatively quickly, the slower dissolution of the silica network ultimately controls the overall reaction rate. This process is further governed by the ratio of the concentration of hydrogen ions (H+) to that of dissolved divalent metal ions. As the pH increases and this ratio decreases, the dissolution of pyroxene slows down. According to Monasterio-Guillot et al. (2021), the specific pyroxene endmember composition influences the efficiency of carbonation reactions, with augite exhibiting greater reactivity with CO2 than diopside. This is attributed to both structural differences and the formation of secondary (more stable) phases such as Fe-oxides and silicates—that lower the system's free energy and promote carbonation. The effect is particularly pronounced in augite due to its higher Fe, Al, and Na content. The study also found that pyroxenes can develop fractures during carbonation, enhancing permeability and fluid infiltration. Such fracturing was shown to be feasible at crustal depths of up to 4 km. The Nordingrå complex contain clinopyroxene but also an abundance of orthopyroxene (12–16%; Table 1). Experimental studies by Oelkers and Schott (2001) demonstrate that enstatite dissolution is strongly pH-dependent, with elevated rates under acidic conditions resulting from protonpromoted exchange at the M2 cation site. This process facilitates the preferential release of Mg and progressive breakdown of the silicate structure (Oelkers and Schott, 2001). Heřmanská et al. (2022) further reported that enstatite dissolves more rapidly than for instance bronzite under acidic conditions, highlighting compositional controls on orthopyroxene reactivity. The orthopyroxene identified in the Nordingrå samples are Fe(II)-bearing and therefore more compositionally comparable to bronzite than to pure enstatite. The overall evaluation of the Nordingrå gabbro indicates promising suitability from both a mineralogical and petrographic perspective. Although it is a layered intrusion—introducing internal compositional variability may also suggest the presence of more mafic components at depth. The degree of alteration within the Nordingrå gabbro is generally low, with a measured MIA of approximately 23.5. Slight variations are observed between samples, with alteration more pronounced near the contact zones. In combination with its mineralogical composition—dominated by pyroxene, calcic plagioclase, and olivine—the Nordingrå gabbro exhibits properties consistent with those required of a viable host rock. Its suitability remains depending on additional site-specific geochemical and structural investigations.

Samples were collected from dolerite outcrops in Örnsköldsvik and the northern parts of Sundsvall (Figure 3). This area, located close to the Nordingrå gabbro-anorthosite complex, hosts several dolerites, occurring as gently dipping sheets that often do not extend deeper than 1,000 m (Lundqvist and Samuelsson, 1973; Hogmalm et al., 2006). Field observations and petrographic analyses indicate that the dolerites

in the study area are only weakly altered. Modal mineralogical analysis (MIA, ~22 samples) revealed minor leaching, and replacement phases were virtually absent across most samples, preserving the primary mineral assemblage. Alteration phases were primarily observed in the two northernmost samples, and otherwise only locally presenttypically confined to fractures and interstitial spaces-suggesting alteration was structurally controlled and limited in extent. Mineralogically, these dolerites exhibit the highest theoretical CO₂ uptake capacity among all case studies (Table 3), owing to their consistently high olivine content (ca. 16.5 vol %) across nearly all sampled outcrops. Notably, the northernmost samples—previously mentioned as exceptions-show elevated chlorite and amphibole content, indicative of more advanced alteration. However, the dolerites might present certain limitations for CO2 injection and storage. Their subsurface geometry and uncertain depth continuity may pose challenges for reservoir development and large-scale injection. Detailed geophysical surveys and structural characterization will be necessary to assess their suitability as storage systems. Taken together, the mineralogical characteristics and strategic location of these dolerites adjacent to the Nordingrå gabbro complex and near major industrial CO₂ point sources—identify the region between Örnsköldsvik and Sundsvall (Figures 3d,e) as a particularly promising target for further assessment of onshore CO₂ storage potential in Sweden.

The Kallax gabbro (Figure 3f) is covering an area of ca. 20 km², and geophysical data indicates a depth of >1,500 meter (Wikström and Söderman, 2000). Actinolite-chlorite replacement of clinopyroxene indicates greenschist to lower amphibolite facies, providing the framework for comparing across the plutonic units in this study. For instance, chlorite is present in all plutonic formations but is most advanced in the Kallax gabbro, where a modal, replacement-based estimate (based on replacive chlorite/replacive chlorite + relict mafic parent) indicates ~37% chloritization of mafic phases. In contrast, the dolerites in Örnsköldsvik/Sundsvall and the Nordingrå gabbro showed only about ~8%. Petrographic observations are also consistent with this. In the Kallax gabbro, chlorite and actinolite commonly replace clinopyroxene, occurring as clevage -and grain internal replacement, along former pyroxene boundaries, and fine aggregates that overprint primary textures. This alteration style also limits fluid access to fresh clinopyroxene and plagioclase cores, blocking reactive Mg-Ca sites and promoting product-layer diffusion control. Consequently, despite still retaining reactive primary components, the effective availability of reactive surfaces is reduced. This alteration has furthermore impacted the theoretical CO₂ uptake of the Kallax gabbro, which show considerably lower values than the other two intrusive rocks (Table 3). Nevertheless, the Kallax gabbro contains a significant amount of clinopyroxene and plagioclase (labradorite) which increases its potential suitability for mineral carbonation compared to the two metavolcanic rocks studied. The Kallax gabbro contains ~12-16% actinolite (Table 1). Although amphibole dissolves much more slowly, it contains both Ca²⁺, Fe2+, and Mg²⁺. Under acidic conditions, actinolite dissolution can be enhanced, but the overall dissolution rate of actinolite seem to be relatively low (10^{-11} .7 mol m⁻² s⁻¹ at ~pH 3, Critelli et al., 2014). Ryu et al. (2011) observed that tremolite exposed to CO₂-rich water at elevated temperatures rapidly precipitated euhedral calcite crystals due to the fast release of Ca, while a Mg-silicate phase (protosaponite) formed more slowly from the residual material. As previously discussed for the metavolcanics, the contribution of minerals like actinolite to carbonation is expected to occur over

extended timescales due to their relatively slow dissolution kinetics. This makes them less compatible with the rapid reaction pathways typically sought in mineral carbonation strategies. Due to the abundance of alteration phases in the Kallax gabbro—many of which partially or fully replace primary minerals—the overall reactive mineralogy is reduced compared to the other subvolcanic/plutonic rocks studied. This suggests that the Kallax gabbro is less favorable for efficient CO_2 mineral storage.

6 Concluding remarks

Storing CO_2 through mineral carbonation deep in the bedrock, in chemically reactive rocks, is one of the fastest and more permanent ways of locking away CO_2 , as the captured gas will convert to mineral form over a (geologically) very short time –a couple of years. This makes mineral storage an interesting addition to offshore CO_2 storage in saline reservoirs beneath the ocean floor.

This study, addressing onshore CO₂ storage as part of climate mitigation techniques, is the first of its kind in Sweden. Here, we have investigated 23 localities through conventional fieldwork, outcrop mapping, sampling, analyses into mineralogy and geochemistry, to assess their theoretical potential for mineral carbonation. This assessment, focused on the reactivity of the rock reservoirs acts as an initial theoretical assessment that admittingly cannot fully address all questions regarding reactivity, dissolution capacity, and the actual carbon sequestration potential of these rocks. However, understanding the reactivity aspect is key in selecting targets for storage, followed by CO₂-uptake experiments (now ongoing) to validate the findings and subsequently, by additional in-depth investigations of the sites, addressing bulk geochemical properties and geometries of the rock reservoirs.

Nevertheless, based on the observed mineralogy, geochemistry and petrology of the studied rocks, data suggests that the theoretically more suitable lithologies are the gabbro-anorthosite complex in Nordingrå and the nearby dolerites around Örnsköldsvik and Sundsvall. These rocks exhibit large proportions of reactive minerals, particularly olivine, as well as substantial amounts of Ca-rich plagioclase and clinopyroxene. In addition, they contain relatively low proportions of alteration minerals, which might otherwise reduce the overall reactivity of the rock. Taken together, these characteristics suggest a favorable potential for ${\rm CO_2}$ mineral storage under appropriate physicochemical conditions, in the Örnsköldsvik-Sundsvall area. Samples from these areas are now being analyzed for their ${\rm CO_2}$ reactivity in a flow-through reactor, and for their porosity/permeability properties.

Data availability statement

The original contributions presented in the study are included in the article/Supplementary material, further inquiries can be directed to the corresponding author.

Author contributions

EC: Data curation, Formal analysis, Investigation, Methodology, Visualization, Writing – original draft, Writing – review & editing. CW: Conceptualization, Funding acquisition, Methodology,

Supervision, Writing – review & editing. GB: Conceptualization, Funding acquisition, Investigation, Methodology, Supervision, Writing – review & editing, Validation.

Funding

The author(s) declare that financial support was received for the research and/or publication of this article. This study was funded by the Swedish Energy Agency (#2020–019943, INSURANCE project, NextGenerationEU) and the packaging company Billerud.

Acknowledgments

The authors would like to extend our thanks to Mathis Warlo for his assistance in the microanalytical work. Special thanks are extended to MSc thesis students Edvard Pearson and Anna Öjebrandt for their dedicated fieldwork and contributions in the Öje, Nordingrå, Sundsvall, and Örnsköldsvik areas. Also, we wish to thank the three reviewers and the editor for significantly improving the manuscript.

Conflict of interest

The authors declare that the research was conducted in the absence of any commercial or financial relationships that could be construed as a potential conflict of interest.

References

Åhman, E., and Wikström, A. (1990). Berggrundskartan 25 M Kalix SO [Bedrock map 25 M Kalix SO]. SGU Serie Ai Nr 45.

Allen, M. R., Dube W, O. P., Solecki, F., Aragón-Durand, W., Cramer, S., Humphreys, M., et al. (2018). "Framing and context supplementary material" in Global warming of 1.5°C. An IPCC special report on the impacts of global warming of 1.5°C above pre-industrial levels and related global greenhouse gas emission pathways, in the context of strengthening the global response to the threat of climate change, sustainable development, and efforts to eradicate poverty. eds. V. Masson-Delmotte, H.-O. Zhai, D. R. Pörtner and J. Skea. Geneva, Switzerland: Intergovernmental Panel on Climate Change (IPCC).

Babechuk, M. G., Widdowson, M., and Kamber, B. S. (2014). Quantifying chemical weathering intensity and trace element release from two contrasting basalt profiles, Deccan traps, India. *Chem. Geol.* 363, 56–75. doi: 10.1016/j.chemgeo.2013.10.027

Berrezueta, E., Moita, P., Pedro, J., Abdoulghafour, H., Mirão, J., Beltrame, M., et al. (2023). Laboratory experiments and modelling of the geochemical interaction of a gabbro-anorthosite with seawater and supercritical CO₂: a mineral carbonation study. *Geoenergy Sci. Eng.* 228:212010. doi: 10.1016/j.geoen.2023.21201

Brantley, S. L., and Chen, Y. (1995). "Chemical weathering rates of pyroxenes and amphiboles" in Chemical weathering rates of silicate minerals. eds. A. F. White and S. L. Brantley (Berlin, Boston: De Gruyter), 119–172.

Clark, D. E., Oelkers, E. H., Gunnarsson, I., Sigfússon, B., Snæbjörnsdóttir, S. Ó., Aradottir, E. S., et al. (2020). Carbfix2: CO_2 and H2S mineralization during 3.5 years of continuous injection into basaltic rocks at more than 250°C. *Geochim. Cosmochim. Acta* 279, 45–66. doi: 10.1016/j.gca.2020.03.039

Critelli, T., Marini, L., Schott, J., Mavromatis, V., Apollaro, C., Rinder, T., et al. (2014). Dissolution rates of actinolite and chlorite from a whole-rock experimental study of metabasalt dissolution from $2 \le pH \le 12$ at 25° C. Chem. Geol. 390, 100–108. doi: 10.1016/j.chemgeo.2014.10.013

Delerce, S. (2023). The reactivity of altered basalts and its implications for natural and engineered carbon mineralization (Doctoral dissertation, Université Paul Sabatier-Toulouse III)

Delerce, S., Bénézeth, P., Schott, J., and Oelkers, E. H. (2023). The dissolution rates of naturally altered basalts at pH 3 and 120°C: implications for the in-situ mineralization of CO₂ injected into the subsurface. *Chem. Geol.* 621:121353. doi: 10.1016/j.chemgeo.2023.121353

Generative AI statement

The author(s) declare that no Gen AI was used in the creation of this manuscript.

Any alternative text (alt text) provided alongside figures in this article has been generated by Frontiers with the support of artificial intelligence and reasonable efforts have been made to ensure accuracy, including review by the authors wherever possible. If you identify any issues, please contact us.

Publisher's note

All claims expressed in this article are solely those of the authors and do not necessarily represent those of their affiliated organizations, or those of the publisher, the editors and the reviewers. Any product that may be evaluated in this article, or claim that may be made by its manufacturer, is not guaranteed or endorsed by the publisher.

Supplementary material

The Supplementary material for this article can be found online at: https://www.frontiersin.org/articles/10.3389/fclim.2025.1685187/full#supplementary-material

Deprez, A., Leadley, P., Dooley, K., Williamson, P., Cramer, W., Gattuso, J., et al. (2024). Sustainability limits needed for CO₂ removal. *Science* 383, 484–486. doi: 10.1126/science.adj6171

Gudbrandsson, S., Wolff-Boenisch, D., Gislason, S. R., and Oelkers, E. H. (2014). Experimental determination of plagioclase dissolution rates as a function of its composition and pH at 22°C. *Geochim. Cosmochim. Acta* 139, 154–172. doi: 10.1016/j.gca.2014.04.028

Heřmanská, M., Voigt, M. J., Marieni, C., Declercq, J., and Oelkers, E. H. (2022). A comprehensive and internally consistent mineral dissolution rate database: part I: primary silicate minerals and glasses. *Chem. Geol.* 597:120807. doi: 10.1016/j.chemgeo.2022.120807

Hogmalm, K. J., Söderlund, U., Larson, S. Å., Meurer, W. P., Hellström, F. A., and Claeson, D. T. (2006). The Ulvö gabbro complex of the 1.27-1.25 ga central Scandinavian dolerite group (CSDG): intrusive age, magmatic setting and metamorphic history. GFF 128, 1–6. doi: 10.1080/11035890601281001

Hughes, C. J. (1973). Spilites, keratophyres, and the igneous spectrum. *Geol. Mag.* 109, 513–527. doi: 10.1017/S0016756800042795

Johnson, N. C., Thomas, B., Maher, K., Rosenbauer, R. J., and Bird, D. (2014). Olivine dissolution and carbonation under conditions relevant for *in situ* carbon storage. *Chem. Geol.* 373, 93–105. doi: 10.1016/j.chemgeo.2014.02.026

Kelemen, P., Benson, S. M., Pilorgé, H., Psarras, P., and Wilcox, J. (2019). An overview of the status and challenges of CO_2 storage in minerals and geological formations. *Front. Clim.* 1:9. doi: 10.3389/fclim.2019.00009

Kelemen, P. B., and Matter, J. (2008). In situ carbonation of peridotite for CO₂ storage. Proc. Natl. Acad. Sci. USA 105, 17295–17300. doi: 10.1073/pnas.0805794105

Lindh, A., Andersson, U. B., Lundqvist, T., and Claesson, S. (2001). Evidence of crustal contamination of mafic rocks associated with rapakivi rocks: an example from the Nordingrå complex. *Central Sweden. Geol. Mag.* 138, 371–386. doi: 10.1017/S0016756801005672

Lundqvist, T. (1987). Berggrundskartan över Västernorrlands län och förutvarande Fjällsjö kommun. SGU Serie Ba Nr 3.

Lundqvist, T., and Samuelsson, L. (1973). The differentiation of a dolerite at Nordingrå, Central Sweden. Sveriges geologiska undersökning C 692, 1–62.

Malmström, M., Banwart, S., Lewenhagen, J., Duro, L., and Bruno, J. (1996). The dissolution of biotite and chlorite at 25° C in the near-neutral pH region. *J. Contam. Hydrol.* 21, 201–213.

Marieni, C., and Oelkers, E. (2018). Carbon sequestration potential of altered mafic reservoirs. *Energy Procedia* 146, 68–73. doi: 10.1016/j.egypro.2018.07.010

Marieni, C., Voigt, M. J., and Oelkers, E. H. (2021). Experimental study of epidote dissolution rates from pH 2 to 11 and temperatures from 25 to 200°C. *Geochim. Cosmochim. Acta* 294, 70–88. doi: 10.1016/j.gca.2020.11.015

Matter, J. M., Speer, J., Day, C., Kelemen, P. B., Ibrahim, A., Mani, S. A., et al. (2025). Rapid mineralisation of carbon dioxide in peridotites. *Commun. Earth Environ.* 6:590. doi: 10.1038/s43247-025-02509-5

Matter, J. M., Stute, M., Snæbjörnsdottir, S. Ó., Oelkers, E. H., Gislason, S. R., Aradottir, E. S., et al. (2016). Rapid carbon mineralization for permanent disposal of anthropogenic carbon dioxide emissions. *Science* 352, 1312–1314. doi: 10.1126/science.aad8132

McGrail, B. P., Schaef, H. T., Spane, F. A., Cliff, J. B., Qafoku, O., Horner, J. A., et al. (2017). Field validation of supercritical $\rm CO_2$ reactivity with basalts. *Environ. Sci. Technol. Lett.* 4, 6–10. doi: 10.1021/acs.estlett.6b00387

Mesfin, K. G., Wolff-Boenisch, D., Gislason, S. R., and Oelkers, E. H. (2023). Effect of cation chloride concentration on the dissolution rates of basaltic glass and labradorite: application to subsurface carbon storage. *Minerals* 13:682. doi: 10.3390/min13050682

Middlemost, E. A. K. (1994). Naming materials in the magma/ igneous rock system. *Earth-Sci. Rev.* 37, 215–224.

Mishra, A., Boon, M. M., Benson, S. M., Watson, M. N., and Haese, R. R. (2023). Reconciling predicted and observed carbon mineralization in siliciclastic formations. *Chem. Geol.* 619:121324. doi: 10.1016/j.chemgeo.2023.121324

Monasterio-Guillot, L., Fernandez-Martinez, A., Ruiz-Agudo, E., and Rodriguez-Navarro, C. (2021). Carbonation of calcium-magnesium pyroxenes: physical-chemical controls and effects of reaction-driven fracturing. *Geochim. Cosmochim. Acta* 304, 258–280. doi: 10.1016/j.gca.2021.02.016

Möri, A., Mazurek, M., Ota, K., Siitari-Kauppi, M., Eichinger, F., and Leuenberger, M. (2021). Quantifying the porosity of crystalline rocks by in situ and laboratory injection methods. *Minerals* 11:1072. doi: 10.3390/min11101072

Neuhoff, P. S., Fridriksson, T., Arnorsson, S., and Bird, D. K. (1999). Porosity evolution and mineral paragenesis during low-grade metamorphism of basaltic lavas at Teigarhorn, eastern Iceland. *Am. J. Sci.* 299, 467–501.

Oelkers, E. H., Gislason, S. R., and Matter, J. (2008). Mineral carbonation of $\rm CO_2$. Elements 4, 333–337. doi: 10.2113/gselements.4.5.333

Oelkers, E. H., Golubev, S. V., Chairat, C., Pokrovsky, O. S., and Schott, J. (2009). The surface chemistry of multi-oxide silicates. *Geochim. Cosmochim. Acta* 73, 4617–4634. doi: 10.1016/j.gca.2009.05.028

Oelkers, E. H., and Schott, J. (2001). An experimental study of enstatite dissolution rates as a function of pH, temperature, and aqueous Mg and Si concentration, and the mechanism of pyroxene/pyroxenoid dissolution. *Geochim. Cosmochim. Acta* 65, 1219–1231. doi: 10.1016/S0016-7037(00)00564-0

Oelkers, E. H., Schott, J., and Devidal, J. L. (1994). The effect of aluminum, pH, and chemical affinity on the rates of aluminosilicate dissolution reactions. *Geochim. Cosmochim. Acta* 58, 2011–2024. doi: 10.1016/0016-7037(94)90281-X

Pearce, J. A. (1996). "A user's guide to basalt discrimination diagrams" in Trace element geochemistry of volcanic rocks: applications for massive sulphide exploration. ed. D. A. Wyman, vol. 12 (Canada: Geological Association of Canada), 79–113.

Ripa, M., and Mellqvist, C. (2012). Beskrivning till erggrundskartan. $V\ddot{a}stra\ delen\ av\ Dalarnas\ l\ddot{a}n$. (SGU K 382), 41–50.

Ryu, K. W., Lee, M. G., and Jang, Y. N. (2011). Mechanism of tremolite carbonation. *Appl. Geochem.* 26, 1215–1221. doi: 10.1016/j.apgeochem.2011.04.010

Seifritz, W. (1990). CO₂ disposal by means of silicates. *Nature* 345:486. doi: 10.1038/345486b0

SGU (Geological Survey of Sweden). (2013). Berggrund 1:50 000 / 1:250 000 – Kartvisare [interactive map]. Sveriges geologiska undersökning. Available online at: https://apps.sgu.se/kartvisare/kartvisare-berg-50-250-tusen.html [Accessed Feb 2024]

Stephens, M. B. (2020). Introduction to the lithotectonic framework of Sweden and organization of this memoir. In Sweden: Lithotectonic framework, tectonic evolution and mineral resources. (Eds.) M. B. Stephens and J. Bergman Weihed. (London: Geological Society of London), 1–18.

Wang, F., Dreisinger, D., Jarvis, M., and Hitchins, T. (2019). Kinetics and mechanism of mineral carbonation of olivine for CO_2 sequestration. *Miner. Eng.* 131, 185–197. doi: 10.1016/j.mineng.2018.11.024

Wikström, A., and Söderman, J. (2000). Berggrundskartan 24
L Luleå NO, skala 1: 50 000. $SGU\,Ai$ 153.

Winchester, J. A., and Floyd, P. A. (1977). Geochemical discrimination of different magma series and their differentiation products using immobile elements. *Chem. Geol.* 20, 325–343.

World Meteorological Organization. (2024). State of the global climate 2023. WMO-no. 1347. ISBN 978-92-63-11347-4. Available online at: https://library.wmo.int/idurl/4/68835 [Accessed Feb, 2025]

Zhu, W., Fusseis, F., Lisabeth, H., Xing, T., Xiao, X., De Andrade, V., et al. (2016). Experimental evidence of reaction-induced fracturing during olivine carbonation. *Geophys. Res. Lett.* 43, 9535–9543. doi: 10.1002/2016GL070834